

Original Article



Hepatic Expression of the Serine Palmitoyltransferase Subunit Sptlc2 Reduces Lipid Droplets in the Liver by Activating VLDL Secretion

Goon-Tae Kim ,¹ Su-Jung Kim ,² Si-Hyun Park ,¹ Dongyup Lee ,¹ Tae-Sik Park ¹

¹Department of Life Science, Gachon University, Seongnam, Korea

²Biomedical Research Center, Asan Institute for Life Sciences, Seoul, Korea



Received: Nov 17, 2019
Revised: Feb 18, 2020
Accepted: Mar 3, 2020

Correspondence to

Tae-Sik Park

Department of Life Science, Gachon University, 1342 Seongnam-daero, Sujeong-gu, Seongnam 13120, Korea.
E-mail: pts9918@gmail.com

Copyright © 2020 The Korean Society of Lipid and Atherosclerosis.

This is an Open Access article distributed under the terms of the Creative Commons Attribution Non-Commercial License (<https://creativecommons.org/licenses/by-nc/4.0/>) which permits unrestricted non-commercial use, distribution, and reproduction in any medium, provided the original work is properly cited.

ORCID iDs

Goon-Tae Kim
<https://orcid.org/0000-0003-0621-0730>
Su-Jung Kim
<https://orcid.org/0000-0001-5729-2129>
Si-Hyun Park
<https://orcid.org/0000-0003-4295-9677>
Dongyup Lee
<https://orcid.org/0000-0002-8653-485X>
Tae-Sik Park
<https://orcid.org/0000-0002-4629-947X>

ABSTRACT

Objective: Ceramide is a signaling molecule that contributes to insulin resistance and hepatosteatosis. In the present study, we activated *de novo* ceramide synthesis by inducing the hepatic expression of Sptlc2 to investigate the role of ceramide in glucose and lipid metabolism.

Methods: We first constructed an adenovirus containing Sptlc2 (AdSptlc2), which encodes a major catalytic subunit of serine palmitoyltransferase (SPT). We then infected hepatocytes and mice fed a regular diet with AdSptlc2 to activate *de novo* ceramide biosynthesis. The liver-specific effects of ceramide biosynthesis on glucose and lipid metabolism were investigated by measuring changes in insulin signaling, lipid droplet formation, and very low-density lipoprotein (VLDL) secretion.

Results: In HepG2 hepatocytes, adenoviral *Sptlc2* expression inhibited insulin signaling and increased ceramide levels via activation of c-Jun N-terminal kinase and serine phosphorylation of insulin receptor substrate 1. In contrast, in mice, AdSptlc2 infection decreased plasma glucose levels by downregulating gluconeogenic genes and increased plasma triglyceride levels by increasing VLDL secretion. In mice infected with AdSptlc2, glucose intolerance and insulin sensitivity improved, while pyruvate utilization via gluconeogenesis decreased.

Conclusion: Hepatic ceramide was found to modulate hepatosteatosis and the insulin response via increased VLDL secretion and inhibition of gluconeogenesis *in vivo*. Although inhibition of the insulin response was observed *in vitro*, the compensatory mechanism of relieving ceramide-induced stress and reducing ceramide levels resulted in improvements of glucose and lipid metabolic profiles *in vivo*. This discrepancy between *in vitro* and *in vivo* regulation mechanisms suggests that ceramide plays a role in non-alcoholic fatty liver disease and insulin resistance.

Keywords: Fatty liver; Lipoprotein; Serine palmitoyltransferase; Ceramides; Gluconeogenesis

Funding

This research was supported by the Bio and Medical Technology Development Program through the National Research Foundation of Korea (NRF), funded by the Korean government (MSIP) (2018M3A9F3020970).

Conflict of Interest

The authors have no conflicts of interest to declare.

Author Contributions

Conceptualization: Park TS; Formal analysis: Kim GT, Kim SJ, Lee D, Park SH; Funding acquisition: Park TS; Investigation: Kim GT, Kim SJ, Lee D, Park SH; Project administration: Park TS; Writing - original draft preparation: Kim GT, Park TS; Writing - review & editing: Park TS.

INTRODUCTION

Obesity is an important risk factor and major cause of metabolic diseases, including diabetes, hyperlipidemia, hypertension, and coronary heart disease.^{1,3} Elevated plasma levels of free fatty acids (FFAs) induces their increased uptake by the liver and the development of non-alcoholic fatty liver.⁴ Elevated levels of FFAs are associated with the occurrence of insulin resistance and diabetes through the disruption of glucose and lipid metabolism in skeletal muscle, liver, and adipose tissue.⁵ In hyperlipidemic conditions caused by excess plasma FFAs, saturated fatty acids (FAs) are utilized to form specific lipid metabolites that can regulate cellular signaling and contribute to lipotoxicity, including lipid-induced organ dysfunction.⁶ These lipid metabolites include diacylglycerol (DAG), ceramide, or their metabolites, which activate serine/threonine kinases or phosphatases that inhibit insulin receptor substrate/protein kinase B (AKT)-dependent insulin-signaling cascades in insulin-sensitive tissues.⁷

Ceramide, a sphingolipid metabolite, is a major component of the plasma membrane and lipoproteins. The *de novo* synthesis of ceramide is initiated by the condensation of serine and palmitoyl CoA. FAs are converted to ceramide via a series of reactions mediated by serine palmitoyltransferase (SPT), 3-ketosphinganine reductase, ceramide synthase, and dihydroceramide desaturase. This *de novo* sphingolipid biosynthesis is activated by excess cellular palmitate under hyperlipidemic conditions in ApoE-deficient liver tissue.^{8,9} Although this pathway is likely to be activated in the settings of obesity and diabetes, the mechanisms underlying its regulation remain unclear.

SPT, which catalyzes the rate-limiting step in the *de novo* ceramide biosynthesis pathway, is composed of 2 main subunits, Sptlc1 and Sptlc2, which encode 53- and 63-kDa proteins, respectively.¹⁰ Deficiency of *Sptlc1* or *Sptlc2* is lethal in mice, and only heterozygous mice or tissue-specific null mice are viable.^{11,12} Although a third SPT subunit, Sptlc3, has been reported, its function needs to be characterized further.¹³ Each SPT subunit is stabilized through the formation of a dimer or multimer in the endoplasmic reticulum, leading to activation of the enzyme and the production of ceramide.¹⁴

Increases in cellular ceramide levels via excessive production of FFAs activate protein phosphatase 2A and dephosphorylate AKT, inhibiting the insulin response.¹⁵ Dephosphorylation of the pleckstrin domain of AKT prevents it from binding to 3-phosphoinositides, which activate AKT.¹⁶ In summary, cellular glucose uptake is reduced by the ceramide-mediated inhibition of insulin signaling. Thus, ceramide synthesis is associated with the development of metabolic dysfunctions, such as insulin resistance, atherosclerosis, cardiomyopathy, and diabetes, and pharmacological or genetic interventions that inhibit ceramide biosynthesis alleviate these metabolic abnormalities.^{17,19}

In this study, we investigated whether hepatic overproduction of ceramide could induce an insulin response. Adenovirus-mediated expression of Sptlc2 greatly increased hepatic ceramide levels, activating c-Jun N-terminal kinase (JNK) and resulting in the phosphorylation of insulin receptor substrate 1 (IRS1) at Ser³¹² in hepatocytes. Independently, increased ceramide levels induced the dephosphorylation of AKT. However, increased hepatic ceramide levels activated hepatic very low-density lipoprotein (VLDL) secretion in the liver of mice overexpressing Sptlc2 and alleviated insulin resistance and impairments in insulin signaling. In summary, our findings indicate that ceramide regulates insulin signaling and VLDL secretion in the liver, depending on its levels.

MATERIALS AND METHODS

1. Materials

Ceramides (C14:0, C16:0, C18:0, C18:1, C20:0, C24:0, C24:1 ceramides), dihydroceramides (C16:0, C18:0, C24:0, C24:1), sphinganine, sphingosine, sphingomyelins (SM; 16:0, C18:0, C18:1), and DAG (C16:0–C16:0, C18:1–C18:1, C16:0–C18:1, C18:0–C18:2, C18:0–C20:4) were obtained from Avanti Polar Lipids (Alabaster, AL, USA). Insulin was obtained from Eli Lilly and Company (Indianapolis, IN, USA).

2. Plasmids and recombinant adenovirus

Construction of recombinant adenoviral vectors (human SPT subunit, adenovirus containing *Sptlc1* [AdSptlc1] and adenovirus containing *Sptlc2* [AdSptlc2]) was performed using the pAdTrack-cytomegalovirus (CMV) vector and the Ad-Easy Adenoviral Vector system (Stratagene, La Jolla, CA, USA). Briefly, cDNAs for full-length *Sptlc1* and *Sptlc2* were generated by polymerase chain reaction (PCR) using specific primers (*Sptlc1* primer, 5'-AAA AGT CGA CTA ACT ATG GCG ACC GCC ACG-3' and 5'-AAA ATC TAG AGG GAA GAG ACA CTG A-3'; *Sptlc2* primer, 5'-AAA ACT CGA GTG CTG CCA GGA AGA TGC-3' and 5'-AAA ATC TAG A CC TCT GAG GGA GCA CCA AAA-3'). The cDNAs were cloned into the pAdTrack-CMV-shuttle vector, which contains a CMV promoter driving the expression of green fluorescent protein (GFP). After selection using kanamycin and confirmation through sequencing, the clones were linearized with PmeI and co-transformed with the adenoviral plasmid pAdEasy-1 in electrocompetent BJ5183 cells.²⁰ Positive clones were selected using ampicillin and confirmed using DNA minipreps and PacI digestion. Recombinant plasmids were linearized using PacI and transfected into HEK 293 cells.²¹ Adenoviruses were purified by the double cesium chloride gradient method.²²

3. Cell culture

HepG2 cells (human hepatocellular carcinoma cells) were obtained from ATCC (Manassas, VA, USA) and cultured in Dulbecco's modified Eagle's medium (DMEM; WelGENE, Gyeongsan, Korea) supplemented with 10% heat-inactivated fetal bovine serum (FBS), 1 U/mL penicillin, and 1 µg/mL streptomycin. The cells were incubated at 37°C under a 5% CO₂ atmosphere. HEK 293 cells (human embryonic kidney cells) were used to generate a recombinant adenovirus and to determine virus titers. The HEK 293 cells were cultured in DMEM supplemented with 10% FBS, 1 U/mL penicillin, and 1 µg/mL streptomycin.

4. Animal experiments

All animal experiments were approved by the Gachon University (Seongnam, Korea) Institutional Animal Care and Use Committee (approval No. LCDI-2015-0013). Eight-week-old male C57Bl/6J mice were purchased from Charles River Laboratories (Wilmington, MA, USA) and fed water and chow *ad libitum* (normal chow diet: Picolab Rodent Diet 20 of LabDiet Inc., St. Louis, MO, USA) in a specific pathogen-free facility at the Gachon Center for Animal Care and Use (12:12 hour light-dark cycle).

For glucose tolerance testing, the mice were subjected to fasting for 16 hours before being given an intraperitoneal injection of glucose (2 g/kg body weight). For insulin tolerance testing, the mice were subjected to fasting for 4 hours and then injected intraperitoneally with insulin (1 U/kg body weight). For pyruvate tolerance testing, the mice were subjected to fasting for 8 hours and then received an intraperitoneal injection of pyruvate (1 g/kg body weight). Blood glucose was measured using blood collected from the tail vein at designated

times. To determine insulin response, insulin (0.5 U/kg body weight) was injected into the mice intraperitoneally for 10 minutes before isolation of the liver. For gene expression and lipid metabolite analyses, the mice were subjected to fasting for 6 hours and their blood and tissues were collected after sacrifice. To measure VLDL secretion, poloxamer-407 was injected intraperitoneally (1 g/kg body weight). Blood was collected from the intraorbital vein at various time points, and triglyceride (TG) levels were measured.

5. Quantitative real-time PCR

Total RNA from mouse primary hepatocytes and HepG2 cells was extracted using the easy-spin (DNA-free) Total RNA Extraction Kit (iNtRON Biotechnology, Inc., Seongnam, Korea), and the mouse livers were homogenized in TRIzol reagent (Invitrogen, Carlsbad, CA, USA). cDNA was synthesized using the iScript cDNA synthesis kit (Bio-RAD, Hercules, CA, USA). Real-time PCR analysis was performed using an ABI7300 instrument (Applied Biosystems Inc, Carlsbad, CA, USA) and SYBR Green Master Mix (Toyobo, Osaka, Japan). The mRNA expression levels of the analyzed genes were normalized to the mRNA levels of β -actin.²³

6. Immunoprecipitation

The cells were lysed in cold lysis buffer (10 mM Tris [pH 7.4], 0.5 mM EDTA, 100 μ M Na₂P₂O₇, 0.5 mM NaF, 1 mM Na₃VO₄, 2% Triton X-100, protease inhibitors, phosphatase inhibitors, and 10% glycerol). To detect phosphotyrosine IRS1, the supernatants (500 μ g of protein) were immunoprecipitated by incubation with an anti-IRS1 antibody (1 μ g) overnight at 4°C and with protein A/G beads for 1 hour at 4°C. The beads were washed twice with PBS and boiled for 10 minutes at 95°C before sodium dodecyl sulfate-polyacrylamide gel electrophoresis (SDS-PAGE) was performed.

7. Western blot analysis

HepG2 cells were grown to 70% confluence in 6-well plates in DMEM. After adenovirus infection, the cells were stimulated with insulin (100 nM/mL) for 10 minutes. Next, the cells were lysed in cold lysis buffer (10 mM Tris [pH 7.4], 0.5 mM EDTA, 100 μ M Na₂P₂O₇, 0.5 mM NaF, 1 mM Na₃VO₄, 2% Triton X-100, protease inhibitor, and phosphatase inhibitors). The immunoprecipitate or 30 μ g of total protein was analyzed using SDS-PAGE and transferred onto a polyvinylidene fluoride membrane. Primary antibodies against phospho-AKT1/PKB (ser473), phospho-protein kinase C (PKC) ϵ (ser729), PKC ϵ , phospho-IRS1 (Tyr612), AKT/PKB, phospho-GSK3 β (ser9), GSK3 β , phospho-JNK, and JNK were purchased from Cell Signaling Technology (Danvers, MA, USA). Antibodies against phospho-insulin R β (Tyr1162/1163), XBPI, and ATF4 (CREB-2) were obtained from Santa Cruz Biotechnology (Dallas, TX, USA). Insulin R β , phospho-IRS1 (Ser307), and IRS1 were purchased from Upstate Biotechnology (Burlington, MA, USA); Sptlc1 from BD Biosciences (Hampton, MA, USA); and Sptlc2 from Abcam (Cambridge, UK). After incubation with horseradish peroxidase-conjugated goat anti-rabbit IgG or goat anti-mouse IgG and IgM (Millipore, Billerica, MA, USA), the blots were developed using an enhanced chemiluminescent substrate (Millipore) and detected using a LAS4000 luminescent image analyzer (Fujifilm, Japan). An antibody against actin (Millipore) was used to normalize the sample loading.

8. Sphingolipid analysis by liquid chromatography with tandem mass spectrometry (LC/MS/MS)

For hepatic lipid analysis, HepG2 cells were seeded at a density of 1×10^6 and incubated at 37°C for 24 hours. After adenovirus infection, the cells were harvested and lysed in lysis buffer. The mouse livers were isolated and homogenized in PBS using TissueLyser II (Qiagen,

Germantown, MD, USA). An internal standard (C17:0-ceramide) was added to the cell extracts containing 1 mg of protein, and sphingolipids were extracted using chloroform/methanol (2:1, v/v) containing 0.01% butylated hydroxytoluene. Ceramides (C14:0, C16:0, C18:0, C18:1, C20:0, C24:0, and C24:1), dihydroceramides (C16:0, C18:0, C24:0, and C24:1), and DAG were separated by high-performance liquid chromatography using a C18 column (XTerra C18, 3.5 μ m, 2.1 \times 50 mm) and ionized in positive electrospray ionization mode, as described by Yoo et al.²⁴ [M⁺]/product ions from the corresponding sphingolipid metabolites were monitored for multiple reaction monitoring quantification, using a bench-top tandem mass spectrometer, API 4000 Q-trap (Applied Biosystems Inc.), interfaced with an electrospray ionization source.

9. Measurement of metabolites

Blood glucose levels under basal conditions and during glucose tolerance tests were measured using an automatic glucose monitor (One Touch; LifeScan, Milpitas, CA, USA). Plasma and hepatic TG, cholesterol, high-density lipoprotein (HDL), low-density lipoprotein (LDL), and non-esterified fatty acid (NEFA) levels were measured using colorimetric assay kits from Wako (Wako Pure Chemical Industries, Ltd., Osaka, Japan).

10. Statistical analysis

Data were generally expressed as mean \pm standard error of the mean. Differences between 2 groups were analyzed using the Student *t*-test. A *p*-value of less than 0.05 was considered to indicate statistical significance.

RESULTS

1. Overexpression of Sptlc2 increased ceramide levels in HepG2 cells

SPT is a rate-limiting enzyme in the *de novo* sphingolipid biosynthetic pathway. To examine the effects of activating *de novo* sphingolipid biosynthesis in hepatocytes, we constructed AdSptlc1 and AdSptlc2. The yield of AdSptlc2 was lower than that of AdSptlc1, most likely due to the cytotoxic effect of ceramide production (data not shown). HepG2 cells were infected with AdSptlc1 or AdSptlc2, and overexpression of each SPT subunit was verified by immunoblot analysis. The expression of the Sptlc1 and Sptlc2 proteins was elevated by AdSptlc1 and AdSptlc2, respectively (**Fig. 1A and B**). Next, to explore whether the increased level of Sptlc2 regulated cellular ceramide levels, we infected HepG2 cells with AdSptlc1 or AdSptlc2 and measured ceramide levels by LC/MS/MS. While ceramide and dihydroceramide levels were elevated as a result of AdSptlc2 infection, AdSptlc1 infection did not alter cellular ceramide levels (**Fig. 1C and D**). These data indicate that although the adenoviral expression of Sptlc1 or Sptlc2 increased the protein level of each SPT subunit, only an increase in Sptlc2 expression increased the production of ceramide in HepG2 cells.

2. Overexpression of Sptlc2 inhibited insulin signaling by increasing phosphorylated JNK (pJNK) levels via the ceramide pathway, but not the DAG pathway

To determine whether adenoviral expression of Sptlc2 inhibited the insulin signaling pathway, we infected HepG2 cells with adenoviruses containing *Sptlc1* or *Sptlc2* and measured the phosphorylation of mitogen activated protein (MAP) kinases and insulin-signaling intermediates. We found that the levels of pJNK were increased by the adenoviral expression of Sptlc2, while no change was caused by infection with AdSptlc1 (**Fig. 2A**). Further, we

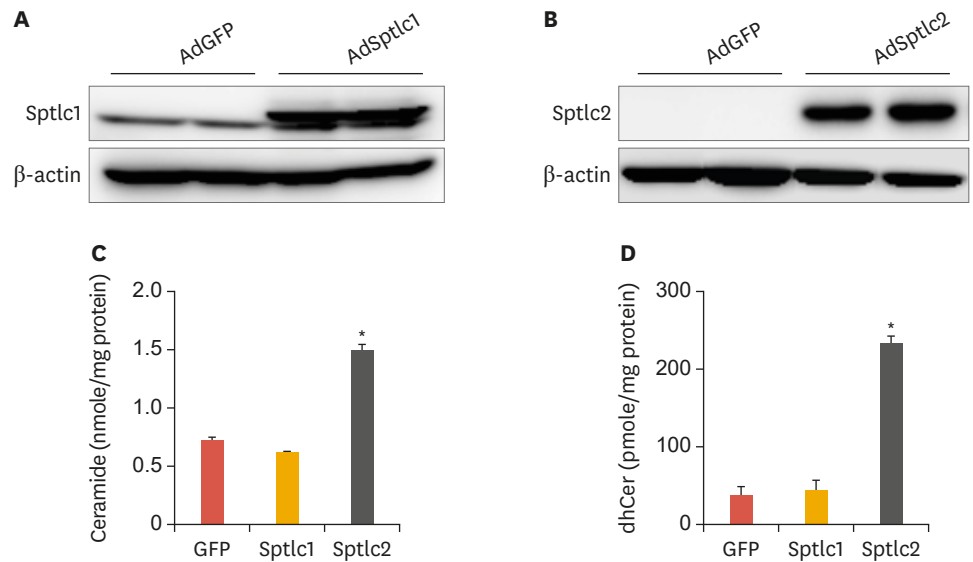


Fig. 1. Adenoviral overexpression of SPT subunits (Sptlc1 and Sptlc2) in HepG2 hepatocytes. Immunoblot analysis of Sptlc1 (A) and Sptlc2 (B) in HepG2 cells infected with AdSptlc1 and AdSptlc2 (multiplicity of infection). Analyses of ceramide (C) and dhCer (D) were performed by LC/MS/MS. Mean±standard error of the mean. SPT, serine palmitoyltransferase; AdSptlc1, adenovirus containing *Sptlc1*; AdSptlc2, adenovirus containing *Sptlc2*; dhCer, dihydroceramide; LC/MS/MS, liquid chromatography with tandem mass spectrometry; GFP, green fluorescent protein. * $p < 0.01$ vs. green fluorescent protein control (n=3).

measured the level of phosphorylated PKC ϵ (pPKC ϵ) on the basis of a previous report indicating that activation of PKC ϵ by DAG inhibited the tyrosine phosphorylation of insulin receptor (IR), leading to inhibition of the insulin-signaling pathway.²⁵ However, in the present study, the AdSptlc2-mediated increase in ceramide levels led to a relative decrease in the level of pPKC ϵ . In contrast, AdSptlc1 did not affect the pPKC ϵ level (Fig. 2A). Cellular DAG levels were not altered by AdSptlc1 or AdSptlc2 (Fig. 2B).

Subsequently, to determine whether the overexpression of Sptlc2 inhibited the insulin-signaling pathway via the phosphorylation of JNK and serine phosphorylation of IRS1, we infected HepG2 cells with an adenovirus containing GFP (AdGFP) or AdSptlc1 or AdSptlc2 and examined the phosphorylation of insulin-signaling mediators. AdSptlc2 reduced serine phosphorylation of AKT and GSK3 β and tyrosine phosphorylation of IRS1 and induced serine phosphorylation of IRS1. In addition, the serine phosphorylation of IR was significantly increased only by AdSptlc2 (Fig. 2C). Unlike AdSptlc2, AdSptlc1 did not affect the phosphorylation of any insulin-signaling mediator when compared with AdGFP (Fig. 2C). These data indicate that the overexpression of Sptlc2 regulated the insulin-signaling pathway by increasing the serine phosphorylation of IR and IRS1. These results suggest that the overexpression of Sptlc2 increased cellular ceramide levels and inhibited the insulin-signaling pathway by the pJNK-mediated serine phosphorylation of IR and IRS1 in HepG2 cells.

3. Adenoviral expression of Sptlc2 reduced lipid accumulation in the liver by increasing VLDL secretion

To examine the effects of activated *de novo* sphingolipid biosynthesis on liver function, mice fed normal chow were injected with AdSptlc2 (5×10^8 PFU) via the tail vein. For the *in vivo* study, we only examined the effects of AdSptlc2, since no effect was observed using AdSptlc1. Fourteen days after the adenovirus injection, we measured the plasma parameters. While we

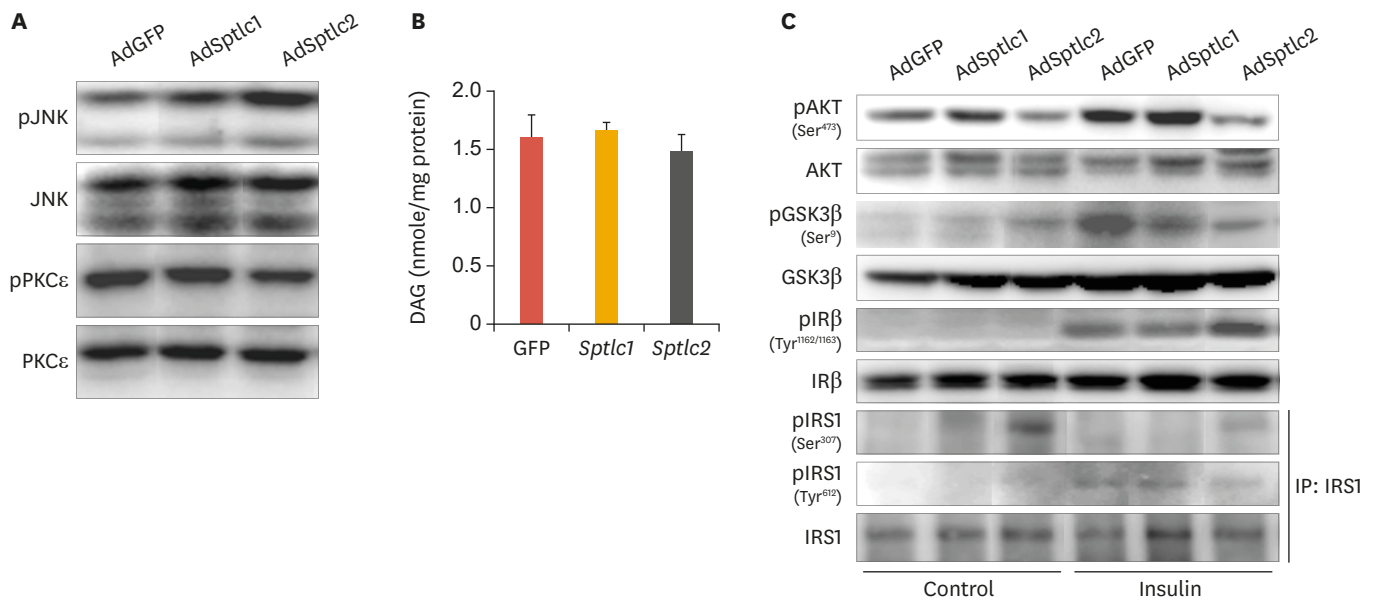


Fig. 2. Adenoviral overexpression of *Sptlc2* activated JNK and caused phosphorylation of IRS1 at Ser³⁰⁷ in HepG2 hepatocytes. Phosphorylation of JNK and PKCε was examined by immunoblot analysis (A). Analyses of DAG were performed by LC/MS/MS (B). Mean±standard error of the mean. After HepG2 cells were infected with AdGFP, Ad*Sptlc1*, or Ad*Sptlc2* (B) overnight, the cells were treated with insulin for 1 hour, and the insulin-signaling intermediates were analyzed by immunoblot analysis (C). IRS1 was immunoprecipitated using an IRS1 antibody, and phosphorylation was evaluated using an antibody against IRS1 phosphorylated at serine or tyrosine.

JNK, c-Jun N-terminal kinase; IRS1, insulin receptor substrate 1; PKC, protein kinase C; DAG, diacylglycerol; LC/MS/MS, liquid chromatography with tandem mass spectrometry; GFP, green fluorescent protein; AdGFP, adenovirus containing green fluorescent protein; AKT, protein kinase B; p-, phosphorylated.

**p*<0.01 vs. green fluorescent protein control (n=3).

did not find any changes in body weight, cholesterol, and HDL, fasting glucose levels were found to be reduced and the TG, LDL, and NEFA levels were found to be elevated (**Table 1**). An analysis of hepatic sphingolipids showed that ceramide, dihydroceramide, and SM levels were all elevated (**Fig. 3A-C**). These results suggest that adenoviral *Sptlc2* expression activates *de novo* sphingolipid synthesis in the liver.

Although hepatic cholesterol levels were not altered, hepatic TG levels were reduced (**Fig. 3D**). To examine whether there was a change in lipid droplet levels in the liver, we stained the liver tissue with Oil Red O. We found fewer hepatic lipid droplets in the Ad*Sptlc2*-injected mice than in the AdGFP-injected controls (**Fig. 3E**). Since the plasma TG levels had increased and the amount of hepatic lipid droplets was reduced in these mice, we questioned whether VLDL secretion was altered by Ad*Sptlc2* infection. Indeed, we found higher TG accumulation in the plasma due to the poloxamer 407 (1 g/kg body weight) injection in the Ad*Sptlc2*-injected mice

Table 1. Hepatic overexpression of *Sptlc2* lowered plasma glucose and elevates plasma TG

	AdGFP (n=8)	Ad <i>Sptlc2</i> (n=8)
Body weight (g)	22±0.5	22.8±0.4
Glucose (mg/dL)	138.3±7.3	70.6±7.3*
TG (mg/dL)	65.7±2.6	115.3±8.7*
Cholesterol (mg/dL)	83.5±1.6	90.5±3.8
HDL-C (mg/dL)	58.3±1.4	54.3±2.7
LDL-C (mg/dL)	5.7±0.3	14.8±0.6*
NEFA (mEq/L)	0.77±0.05	1.05±0.07*

Mean±standard error of the mean.

AdGFP, adenovirus containing green fluorescent protein; Ad*Sptlc2*, adenovirus containing *Sptlc2*; TG, triglyceride; HDL-C, high-density lipoprotein cholesterol, LDL-C, low-density lipoprotein cholesterol; NEFA, elevated nonesterified fatty acids.

**p*<0.05 vs. AdGFP (n=8).

Ceramide and Hepatic VLDL Secretion

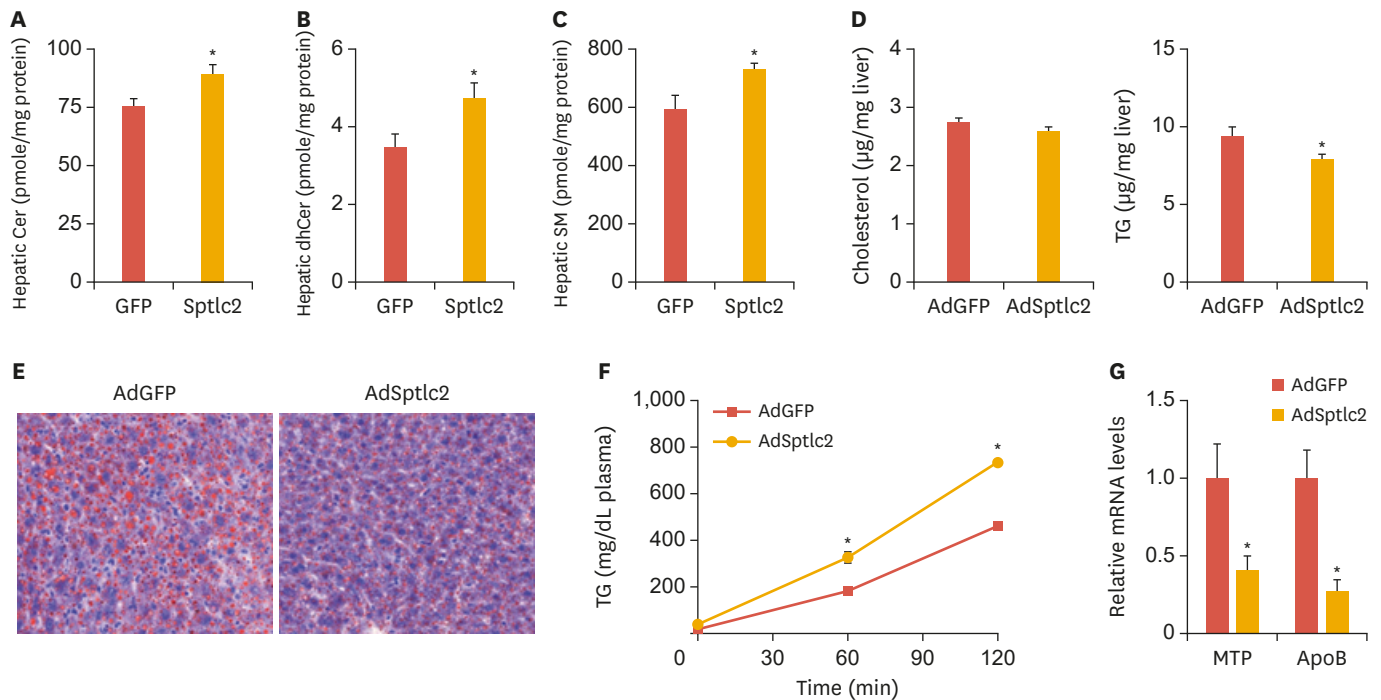


Fig. 3. Adenoviral overexpression of *Sptlc2* elevated sphingolipid levels, reduced the amount of lipid droplets, and activated VLDL secretion in mice fed regular chow. Mice fed regular chow were infected with AdGFP or AdSptlc2 via a tail-vein injection (1×10^9 PFU). After 2 weeks, the liver was removed and Cer (A), dhCer (B), and SM (C) levels were analyzed by LC/MS/MS. Hepatic cholesterol and TG levels were measured by a colorimetric assay, as described in the Materials and Methods section (D). The liver sections were stained with Oil Red O (E). After poloxamer 407 was injected into the mice intraperitoneally, their blood was collected at various time points and their plasma TG levels were measured (F). MTP and ApoB mRNA was measured by real-time polymerase chain reaction (G). Mean \pm standard error of the mean.

VLDL, very low-density lipoprotein; AdGFP, adenovirus containing green fluorescent protein; AdSptlc2, adenovirus containing *Sptlc2*; Cer, ceramide; dhCer, dihydroceramide; SM, sphingomyelin; LC/MS/MS, liquid Chromatography with tandem mass spectrometry; TG, triglyceride; MTP, microsomal triglyceride transfer protein; ApoB, apolipoprotein B.

* $p < 0.05$ vs green fluorescent protein control (n=5).

(Fig. 3F). In addition, we measured the expression of genes involved in VLDL secretion, such as the genes encoding microsomal triglyceride transfer protein (MTP) and apolipoprotein B (ApoB). However, the mRNA levels of MTP and ApoB were noticeably reduced in the liver of the AdSptlc2-injected mice (Fig. 3G). These results suggest that hepatic overexpression of *Sptlc2* and activation of *de novo* sphingolipid biosynthesis activated hepatic VLDL secretion and reduced the amount of hepatic lipid droplets.

4. Adenoviral expression of *Sptlc2* improved glucose and insulin sensitivity

Next, we explored whether glucose metabolism was affected by the activation of *de novo* sphingolipid biosynthesis in the liver. Fasting glucose levels were lower and the glucose response was more sensitive in AdSptlc2 mice (Fig. 4A and Table 1). To examine gluconeogenesis in the liver, we performed pyruvate tolerance testing and found that gluconeogenesis was suppressed in AdSptlc2-injected mice (Fig. 4B). In addition, the insulin response was more sensitive in AdSptlc2-injected mice (Fig. 4C).

To further explore these results, we analyzed the degree of phosphorylation of insulin-signaling intermediates. We found increased levels of phosphorylated AKT (pAKT) and pGSK3 β in response to insulin (Fig. 5A). In addition, the expression of gluconeogenic genes, including glucose 6-phosphatase (G6Pase) and phosphoenolpyruvate carboxykinase (PEPCK), were downregulated in the liver of AdSptlc2-injected mice (Fig. 5B). These results

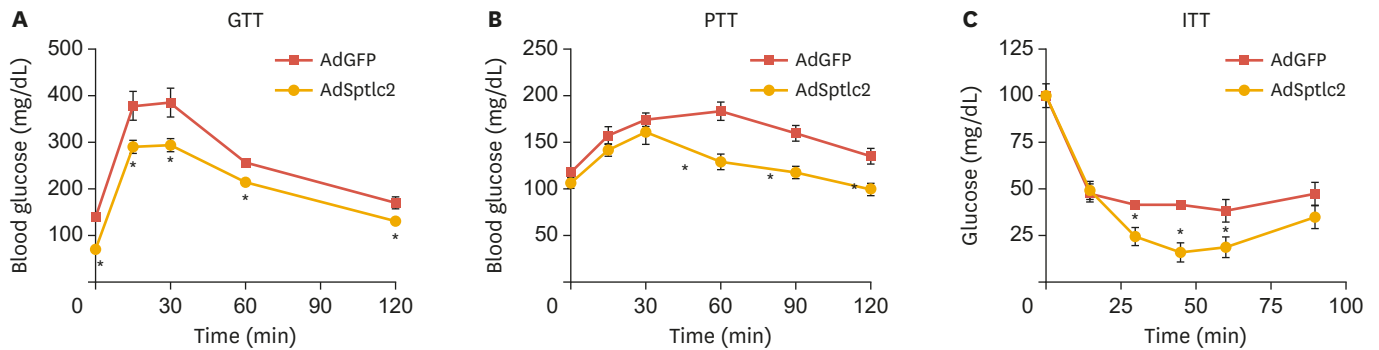


Fig. 4. Adenoviral overexpression of *Sptlc2* improved glucose tolerance, pyruvate tolerance, and insulin intolerance. Mice fed regular chow were infected with AdGFP or AdSptlc2 via a tail-vein injection (1×10^9 PFU). After 2 weeks, a GTT (A), PTT (B), and ITT (C) were performed. At various time points, blood was collected, and the glucose levels in the blood were measured, as described in the Materials and Methods section. Mean \pm standard error of the mean. AdGFP, adenovirus containing green fluorescent protein; AdSptlc2, adenovirus containing *Sptlc2*; GTT, glucose tolerance test; PTT, pyruvate tolerance test; ITT, insulin tolerance test. * $p < 0.05$ vs. green fluorescent protein control ($n=5$).

suggest that the activation of *de novo* sphingolipid biosynthesis by AdSptlc2 improved sensitivity to glucose and insulin and inhibited gluconeogenesis.

DISCUSSION

Sphingolipids are essential components of the plasma membrane and lipoproteins. Ceramide is a sphingolipid metabolite involved in the development of insulin resistance and metabolic dysfunction.^{26,27} When ceramide accumulates in tissues, including the liver, skeletal muscle, and heart, metabolic dysfunction occurs and contributes to the development of hepatosteatosis, diabetes, and dilated cardiomyopathy.^{18,19,27} In this study, we investigated the effects of activated *de novo* sphingolipid biosynthesis on hepatic lipid and glucose metabolism. We observed the following results: 1) adenoviral expression of *Sptlc2* increased ceramide levels, which inhibited the insulin-signaling response through JNK activation, 2) increased ceramide levels in the liver activated VLDL secretion, 3) the insulin response was

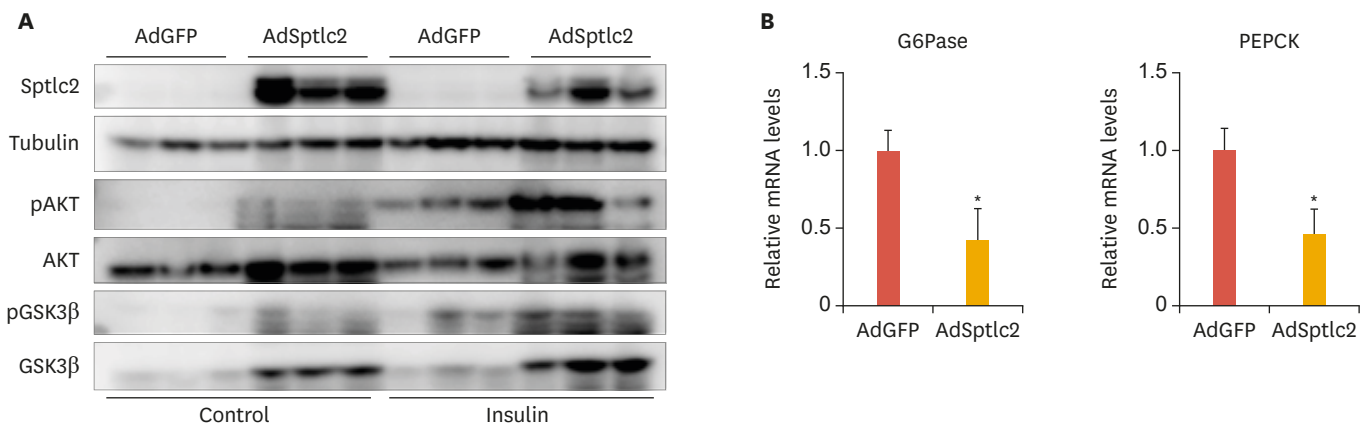


Fig. 5. Adenoviral overexpression of *Sptlc2* increased the sensitivity of insulin signaling and suppressed gluconeogenic genes. Mice fed regular chow were infected with AdGFP or AdSptlc2 via a tail-vein injection (1×10^9 PFU). After 2 weeks, the insulin response was measured by immunoblotting the signaling intermediates (A). Expression of gluconeogenic genes, including those encoding G6Pase and PEPCK, was measured by real-time polymerase chain reaction (B). Mean \pm standard error of the mean. AdGFP, adenovirus containing green fluorescent protein; AdSptlc2, adenovirus containing *Sptlc2*; G6pase, glucose 6-; PEPCK, phosphoenolpyruvate carboxykinase. * $p < 0.05$ vs. green fluorescent protein control ($n=5$).

improved by Sptlc2 expression, and 4) reduced gluconeogenesis contributed to reduced blood glucose levels.

Sphingolipids are basic cellular structural and signaling molecules. Among them, ceramide has been studied extensively in cancer and metabolic research.^{16, 28-30} *De novo* ceramide biosynthesis has been established as a cause of insulin resistance. Inhibition of *de novo* ceramide synthesis ameliorates glucose intolerance in heterozygous *Sptlc2*-deficient mice and diet-induced obese mice.^{31, 32} Although those findings suggest that *de novo* ceramide production mediated by SPT contributes to hepatic dysfunction, the effects of ceramide on liver function have not been studied well.

Surprisingly, the adenoviral overexpression of *Sptlc2* demonstrated contrasting results *in vitro* and *in vivo*. A previous study showed that JNK and JNK-mediated serine phosphorylation of IRS1 led to insulin resistance.³³ Consistent with these findings, we found that an increase in the ceramide level in HepG2 hepatocytes via Ad*Sptlc2* overexpression activated JNK, which phosphorylated IRS1 at Ser³⁰⁷. Previous reports have demonstrated that exogenous and endogenous ceramides cause JNK activation.³⁴ These findings indicate that insulin signaling is inhibited by ceramide production via JNK activation (**Fig. 2**). Increments in ceramide levels decreased pAKT, possibly via protein phosphatase 2A.²⁸ In contrast with the results observed in cells in the present study and those reported previously, the mice injected with Ad*Sptlc2* exhibited increased insulin sensitivity despite having elevated ceramide levels. Additionally, hepatic fat accumulation was reduced in these mice, which might have been mainly due to increased hepatic VLDL secretion. Consistent with this result, the hepatic expression of *Sptlc2* elevated plasma TG and LDL cholesterol (**Table 1**). These results suggest that hepatic ceramide levels might have exceeded the threshold of acceptable levels due to the extreme increment. The liver secretes more VLDL into the bloodstream to remove excess “lipotoxic” sphingolipids, including ceramide; thus, VLDL secretion relieves ceramide-induced stress, acting as a defense mechanism. Therefore, ceramide regulates insulin sensitivity and VLDL secretion differently, depending on the ceramide level in the liver. Within a physiologically relevant range of ceramide levels, ceramide mainly regulates the sensitivity of the insulin response, rather than VLDL secretion. Since the mechanism by which ceramide switches between the regulation of insulin signaling and the regulation of VLDL secretion is not yet known, further studies should be conducted of this issue using genetic animal models.

Fasting blood glucose levels in the mice injected with Ad*Sptlc2* were lower than those in the control mice (**Table 1**). This is an unexpected result, since previous reports suggested that increased ceramide levels inhibit insulin signaling and contribute to the occurrence of insulin resistance.¹⁸ This could have mainly been due to the relief of ceramide-induced stress by activation of VLDL secretion resulting from the increase in ceramide. The observation that hepatic gluconeogenic genes, including G6Pase and PEPCK, were downregulated suggests that increased VLDL secretion in response to the drastic accumulation of ceramide contributed to decreased plasma glucose levels via the inhibition of hepatic gluconeogenesis (**Fig. 5**).

In this study, we utilized mice fed normal chow to characterize only the effect of ceramide on liver function. The commonly used high-fat diet also increases levels of other lipid metabolites, including DAG and saturated fatty acids. Indeed, cellular DAG levels were not altered and PKC ϵ -mediated inhibition of insulin signaling was excluded. However, we found a reduction in pPKC ϵ . In contrast, pJNK was present at increased levels and found to be involved in the inhibition of the insulin response. A previous study reported that myriocin,

an SPT inhibitor, inhibited JNK signaling in rats fed a high-fat diet.³⁵ Therefore, ceramide is a major modulator of JNK, rather than PKC ϵ , for IRS1 regulation. Additionally, the amount of lipid droplets in the liver of the mice was reduced. Although our experimental conditions were not hyperlipidemic, the increased release of VLDL from the liver suggests that the reduction in the amount of lipid droplets was mainly due to increased hepatic ceramide levels. Indeed, a recent report suggested that decreased hepatic ceramide levels caused by the inhibition of dihydroceramide desaturase 1 alleviate hepatosteatosis and insulin resistance.²⁷ A detailed study should be performed to elucidate the role of ceramide or other sphingolipid metabolites in the link between hepatosteatosis and VLDL metabolism.

In conclusion, we found that hepatic ceramide regulated hepatosteatosis and the insulin response via inhibition of gluconeogenesis and VLDL secretion. This regulation through sphingolipids might primarily occur through the reduction of stress on the liver via VLDL secretion. Since lipids such as triacylglycerols and ceramides inflict major insults on the liver, the liver could compensate for these insults by reducing its lipid levels. The altered signaling revealed in this study could play an important role in hepatic lipid metabolism in the AdSptlc2-infected mice. Activation of the fatty-acid oxidation pathway and VLDL secretion ameliorated the pathophysiological conditions caused by the activation of *de novo* sphingolipid biosynthesis in the liver. This regulatory mechanism provides support for the role of ceramide in non-alcoholic fatty liver disease and will contribute to the development of therapeutic interventions.

REFERENCES

1. Barr EL, Cameron AJ, Balkau B, Zimmet PZ, Welborn TA, Tonkin AM, et al. HOMA insulin sensitivity index and the risk of all-cause mortality and cardiovascular disease events in the general population: the Australian Diabetes, Obesity and Lifestyle Study (AusDiab) study. *Diabetologia* 2010;53:79-88.
[PUBMED](#) | [CROSSREF](#)
2. Hastie CE, Padmanabhan S, Slack R, Pell AC, Oldroyd KG, Flapan AD, et al. Obesity paradox in a cohort of 4880 consecutive patients undergoing percutaneous coronary intervention. *Eur Heart J* 2010;31:222-226.
[PUBMED](#) | [CROSSREF](#)
3. Roberts AW, Clark AL, Witte KK. Review article: left ventricular dysfunction and heart failure in metabolic syndrome and diabetes without overt coronary artery disease--do we need to screen our patients? *Diab Vasc Dis Res* 2009;6:153-163.
[PUBMED](#) | [CROSSREF](#)
4. Bradbury MW. Lipid metabolism and liver inflammation. I. Hepatic fatty acid uptake: possible role in steatosis. *Am J Physiol Gastrointest Liver Physiol* 2006;290:G194-G198.
[PUBMED](#) | [CROSSREF](#)
5. Unger RH. Lipid overload and overflow: metabolic trauma and the metabolic syndrome. *Trends Endocrinol Metab* 2003;14:398-403.
[PUBMED](#) | [CROSSREF](#)
6. Listenberger LL, Han X, Lewis SE, Cases S, Farese RV Jr, Ory DS, et al. Triglyceride accumulation protects against fatty acid-induced lipotoxicity. *Proc Natl Acad Sci U S A* 2003;100:3077-3082.
[PUBMED](#) | [CROSSREF](#)
7. Jaeschke A, Davis RJ. Metabolic stress signaling mediated by mixed-lineage kinases. *Mol Cell* 2007;27:498-508.
[PUBMED](#) | [CROSSREF](#)
8. Jeong T, Schissel SL, Tabas I, Pownall HJ, Tall AR, Jiang X. Increased sphingomyelin content of plasma lipoproteins in apolipoprotein E knockout mice reflects combined production and catabolic defects and enhances reactivity with mammalian sphingomyelinase. *J Clin Invest* 1998;101:905-912.
[PUBMED](#) | [CROSSREF](#)
9. Hanada K. Serine palmitoyltransferase, a key enzyme of sphingolipid metabolism. *Biochim Biophys Acta* 2003;1632:16-30.
[PUBMED](#) | [CROSSREF](#)

10. Weiss B, Stoffel W. Human and murine serine-palmitoyl-CoA transferase--cloning, expression and characterization of the key enzyme in sphingolipid synthesis. *Eur J Biochem* 1997;249:239-247.
[PUBMED](#) | [CROSSREF](#)
11. Hojjati MR, Li Z, Jiang XC. Serine palmitoyl-CoA transferase (SPT) deficiency and sphingolipid levels in mice. *Biochim Biophys Acta* 2005;1737:44-51.
[PUBMED](#) | [CROSSREF](#)
12. Li Z, Li Y, Chakraborty M, Fan Y, Bui HH, Peake DA, et al. Liver-specific deficiency of serine palmitoyltransferase subunit 2 decreases plasma sphingomyelin and increases apolipoprotein E levels. *J Biol Chem* 2009;284:27010-27019.
[PUBMED](#) | [CROSSREF](#)
13. Hornemann T, Richard S, Rützi MF, Wei Y, von Eckardstein A. Cloning and initial characterization of a new subunit for mammalian serine-palmitoyltransferase. *J Biol Chem* 2006;281:37275-37281.
[PUBMED](#) | [CROSSREF](#)
14. Hornemann T, Wei Y, von Eckardstein A. Is the mammalian serine palmitoyltransferase a high-molecular-mass complex? *Biochem J* 2007;405:157-164.
[PUBMED](#) | [CROSSREF](#)
15. Stratford S, Hoehn KL, Liu F, Summers SA. Regulation of insulin action by ceramide: dual mechanisms linking ceramide accumulation to the inhibition of Akt/protein kinase B. *J Biol Chem* 2004;279:36608-36615.
[PUBMED](#) | [CROSSREF](#)
16. Holland WL, Summers SA. Sphingolipids, insulin resistance, and metabolic disease: new insights from *in vivo* manipulation of sphingolipid metabolism. *Endocr Rev* 2008;29:381-402.
[PUBMED](#) | [CROSSREF](#)
17. Park TS, Panek RL, Mueller SB, Hanselman JC, Rosebury WS, Robertson AW, et al. Inhibition of sphingomyelin synthesis reduces atherogenesis in apolipoprotein E-knockout mice. *Circulation* 2004;110:3465-3471.
[PUBMED](#) | [CROSSREF](#)
18. Holland WL, Brozinick JT, Wang LP, Hawkins ED, Sargent KM, Liu Y, et al. Inhibition of ceramide synthesis ameliorates glucocorticoid-, saturated-fat-, and obesity-induced insulin resistance. *Cell Metab* 2007;5:167-179.
[PUBMED](#) | [CROSSREF](#)
19. Park TS, Hu Y, Noh HL, Drosatos K, Okajima K, Buchanan J, et al. Ceramide is a cardiotoxin in lipotoxic cardiomyopathy. *J Lipid Res* 2008;49:2101-2112.
[PUBMED](#) | [CROSSREF](#)
20. Cheng GC, Schulze PC, Lee RT, Sylvan J, Zetter BR, Huang H. Oxidative stress and thioredoxin-interacting protein promote intravasation of melanoma cells. *Exp Cell Res* 2004;300:297-307.
[PUBMED](#) | [CROSSREF](#)
21. He TC, Zhou S, da Costa LT, Yu J, Kinzler KW, Vogelstein B. A simplified system for generating recombinant adenoviruses. *Proc Natl Acad Sci U S A* 1998;95:2509-2514.
[PUBMED](#) | [CROSSREF](#)
22. Duffy AM, O'Doherty AM, O'Brien T, Strappe PM. Purification of adenovirus and adeno-associated virus: comparison of novel membrane-based technology to conventional techniques. *Gene Ther* 2005;12 Suppl 1:S62-S72.
[PUBMED](#) | [CROSSREF](#)
23. Chang ZQ, Lee SY, Kim HJ, Kim JR, Kim SJ, Hong IK, et al. Endotoxin activates de novo sphingolipid biosynthesis via nuclear factor kappa B-mediated upregulation of *Sptlc2*. *Prostaglandins Other Lipid Mediat* 2011;94:44-52.
[PUBMED](#) | [CROSSREF](#)
24. Yoo HH, Son J, Kim DH. Liquid chromatography-tandem mass spectrometric determination of ceramides and related lipid species in cellular extracts. *J Chromatogr B Analyt Technol Biomed Life Sci* 2006;843:327-333.
[PUBMED](#) | [CROSSREF](#)
25. Ryu D, Oh KJ, Jo HY, Hedrick S, Kim YN, Hwang YJ, et al. TORC2 regulates hepatic insulin signaling via a mammalian phosphatidic acid phosphatase, LIPIN1. *Cell Metab* 2009;9:240-251.
[PUBMED](#) | [CROSSREF](#)
26. Hotamisligil GS. Endoplasmic reticulum stress and the inflammatory basis of metabolic disease. *Cell* 2010;140:900-917.
[PUBMED](#) | [CROSSREF](#)
27. Chaurasia B, Tippetts TS, Mayoral Monibas R, Liu J, Li Y, Wang L, et al. Targeting a ceramide double bond improves insulin resistance and hepatic steatosis. *Science* 2019;365:386-392.
[PUBMED](#) | [CROSSREF](#)

28. Pettus BJ, Chalfant CE, Hannun YA. Ceramide in apoptosis: an overview and current perspectives. *Biochim Biophys Acta* 2002;1585:114-125.
[PUBMED](#) | [CROSSREF](#)
29. Oskouian B, Saba JD. Cancer treatment strategies targeting sphingolipid metabolism. *Adv Exp Med Biol* 2010;688:185-205.
[PUBMED](#) | [CROSSREF](#)
30. Bartke N, Hannun YA. Bioactive sphingolipids: metabolism and function. *J Lipid Res* 2009;50 Suppl:S91-S96.
[PUBMED](#) | [CROSSREF](#)
31. Ussher JR, Koves TR, Cadete VJ, Zhang L, Jaswal JS, Swyrd SJ, et al. Inhibition of de novo ceramide synthesis reverses diet-induced insulin resistance and enhances whole-body oxygen consumption. *Diabetes* 2010;59:2453-2464.
[PUBMED](#) | [CROSSREF](#)
32. Li Z, Zhang H, Liu J, Liang CP, Li Y, Li Y, et al. Reducing plasma membrane sphingomyelin increases insulin sensitivity. *Mol Cell Biol* 2011;31:4205-4218.
[PUBMED](#) | [CROSSREF](#)
33. Hirosumi J, Tuncman G, Chang L, Görgün CZ, Uysal KT, Maeda K, et al. A central role for JNK in obesity and insulin resistance. *Nature* 2002;420:333-336.
[PUBMED](#) | [CROSSREF](#)
34. Morad SA, Cabot MC. Ceramide-orchestrated signalling in cancer cells. *Nat Rev Cancer* 2013;13:51-65.
[PUBMED](#) | [CROSSREF](#)
35. Jiang M, Li C, Liu Q, Wang A, Lei M. Inhibiting ceramide synthesis attenuates hepatic steatosis and fibrosis in rats with non-alcoholic fatty liver disease. *Front Endocrinol (Lausanne)* 2019;10:665.
[PUBMED](#) | [CROSSREF](#)